HHS Public Access

Author manuscript

AJNR Am J Neuroradiol. Author manuscript; available in PMC 2018 January 01.

Published in final edited form as:

AJNR Am J Neuroradiol. 2017 July ; 38(7): 1328–1334. doi:10.3174/ajnr.A5180.

Diffusional Kurtosis Imaging and Motor Outcome in Acute Ischemic Stroke

Maria Vittoria Spampinato[1,2], **Clifford Chan**[1,2], **Jens H. Jensen**[1,2], **Joseph A. Helpern**[1,2,5], **Leonardo Bonilha**[5], **Steven A. Kautz**[3,6], **Paul J. Nietert**[4], and **Wuwei Feng**[4,5]

[1]Department of Radiology and Radiological Science, Medical University of South Carolina, Charleston, SC, USA

[2]Center for Biomedical Imaging, Medical University of South Carolina, Charleston, SC, USA

[3]Department of Health Sciences and Research, Medical University of South Carolina, Charleston, SC, USA

[4]Department of Public Health Sciences, Medical University of South Carolina, Charleston, SC, USA

[5]Department of Neurology, Medical University of South Carolina, Charleston, SC, USA

[6]Ralph H. Johnson VA Medical Center, Charleston, SC, USA

Abstract

Background and Purpose—To evaluate whether diffusional kurtosis imaging (DKI) can detect corticospinal tract (CST) microstructural changes in the acute phase for patients with first-ever ischemic stroke and motor impairment, and to assess the correlations between DKI-derived diffusion metrics for the CST and motor impairment 3 months post-stroke.

Materials and Methods—We evaluated seventeen stroke patients who underwent a brain MRI including DKI within four days after the onset of symptoms. Neurological evaluation included the Fugl-Meyer Motor Upper Extremity scale (FM-UE) in the acute phase and 3 months post-stroke. For the CST in the lesioned and contralateral hemispheres, we estimated with DKI both pure diffusion metrics, such as the mean diffusivity and mean kurtosis, as well as model-dependent quantities, such as the axonal water fraction. We evaluated the correlations between CST diffusion metrics and FM-UE at 3 months.

Results—Among all the diffusion metrics, the largest percent signal changes of the lesioned hemisphere CST were observed using axial kurtosis, with an average 12% increase compared to the contralateral CST. The strongest associations between 3-month FM-UE and diffusion metrics were found for the lesioned / contralateral hemisphere CST mean kurtosis (rho = − 0.85) and axial kurtosis (rho = − 0.78) ratios.

Corresponding Author: Maria Vittoria Spampinato, MD, Department of Radiology and Radiological Science, Medical University of South Carolina, 96 Jonathan Lucas, MSC 323, Charleston, SC 29425, Phone: (843) 792 0209, Fax: (843) 792 792-1767, spampin@musc.edu, Twitter handle: @mvspampinato.

Presentation at meetings: None at the time of manuscript submission.

Conclusion—This study was designed to be one of hypothesis generation. Diffusion metrics related to the kurtosis were found to be more sensitive than conventional diffusivity metrics to early post-stroke CST microstructural changes and may have potential value in the prediction of motor impairment at 3 months.

Introduction

Motor impairment caused by injury of the motor pathways is the most common deficit after stroke[1]. While a proportion of acute stroke patients exhibiting motor deficit will have functional recovery, the degree of motor recovery is highly variable[2]. Clinical assessment of motor impairment in the acute phase is a significant predictor of chronic motor outcome[3]. However, for patients with severe initial motor impairment, long-term motor outcome is only weakly predicted by the degree of motor impairment in the acute phase[4]. Thus, it remains difficult to make an accurate motor outcome prediction for an individual patient using information collected in the acute phase. If clinicians had access to an early marker of motor pathways injury and were able to predict motor outcome, stroke recovery could be greatly improved by delivering treatments to those individuals who are likely to benefit from intervention.

The integrity of the corticospinal tract (CST) is critical for recovery of motor function in stroke[5]. Identification of early CST microstructural changes in acute stroke patients would improve our ability to predict motor recovery and plan rehabilitative treatments. DTI can quantify early CST microstructural changes in stroke patients with motor impairment[6–10]. However, one limitation of DTI is that the data analysis approximates the water diffusion dynamics within brain tissue as being a Gaussian process, although significant non-Gaussian diffusion effects are observed throughout the brain. Hence, DTI does not fully characterize water diffusion in the brain. Diffusional kurtosis imaging (DKI) is a clinically feasible diffusion MRI method, which extends the DTI model to include non-Gaussian diffusion effects[11, 12]. As a result, DKI has the potential to provide more sensitive biomarkers for probing microscopic structural changes[13]. In addition, white matter tract integrity (WMTI) metrics can be obtained from the DKI dataset using a model that describes the microstructural characteristics in the extra- and intra-axonal compartments of the WM[14]. To our knowledge, no prospective studies have previously assessed the role of DKI in the prediction of motor outcome after stroke.

Our objectives were to evaluate whether DKI-derived diffusion metrics can detect early CST microstructural changes 1–4 days after first-ever acute ischemic stroke and motor impairment, and to assess the correlations between CST DKI-derived metrics and 3-month motor outcome measured using the Fugl-Meyer Motor Scale Upper Extremity Scale (FM-UE).

Methods

Subjects

The local Institutional Review Board approved the study. Patients with first-ever ischemic stroke with various degrees of motor impairment were enrolled in this prospective

observational study. Written informed consent was obtained from all patients or their legal representatives. Inclusion criteria were the following: 1. Age between 18 and 80 years; 2. First-ever ischemic stroke involving only one hemisphere, confirmed by MRI; 3. Brain MRI, including DKI, obtained between 1 and 4 days after stroke onset; 4. Pre-stroke mRS ≤1; 5. Unilateral motor impairment at baseline with FM-UE score ≤56 out of 66 (to avoid recovery ceiling effect). We excluded any subject with intracranial hemorrhage, other neurological disorders affecting limb motor function, severe dementia, recurrent stroke or death during the 3-month follow-up.

A detailed neurological examination was performed by a stroke neurologist in the acute phase and at a 3-month follow-up visit. The baseline examination included the FM-UE and the NIHSS (Table 1). During the 3-month follow-up examination the FM-UE, NIHSS, and mRS were obtained. The FM-UE Scale, a motor assessment scale with excellent intra- and inter-rater reliability, represented the primary motor outcome variable (maximum score is 66 points, higher scores indicate less severe impairment)[15]. We also calculated the percent change of the FM-UE scale between the baseline and 3-month evaluation. For descriptive purposes, patients were divided into 3 cohorts based on the 3-month FM-UE scale: (1) Upper limb remained essentially plegic (FM-UE ≤ 9); (2) Patients with well-defined upper limb mass flexion and extension synergy-dependent movements (FM-UE = 10 to 18); (3) Patients with recovery of isolated upper limb movements (FM-UE ≥ 19)[16]. We also recorded the total number of days each patient received rehabilitative therapy (including physical therapy and/or occupational therapy during rehabilitation, at home and during outpatient visits) between the stroke and the 3-month follow-up.

Imaging

Brain MRIs were performed on a 1.5 Tesla MRI scanner. A sagittal T1-weighted MPRAGE (voxel size 1 × 1 × 1 mm^3) sequence was obtained. Axial diffusion-weighted images were acquired with 3 b-values (0, 1000 and 2000 s/mm^2) along 30 diffusion encoding directions using a single-shot twice-refocused spin-echo EPI sequence with NEX = 1 (NEX = 10 for b = 0). Imaging parameters of the diffusion sequence were the following: voxel size = 3 × 3 × 3 mm^3, number of slices = 40, TR/TE = 5500/99 ms, field-of-view = 222 × 222 mm^2, acquisition matrix = 74 × 74, BW/pixel = 1325 Hz, acceleration factor = 2, acquisition time ≈ 7 minutes.

Using Diffusional Kurtosis Estimator software[17] (version 2.6, https://www.nitrc.org/projects/dke/), implemented in MATLAB (MathWorks, Natick, MA), the diffusion and kurtosis tensors were calculated on a voxel-by-voxel basis. Parametric maps for the following metrics were obtained from the DKI data set: 1. Diffusivity metrics: fractional anisotropy (FA), mean diffusivity (MD), axial ($\lambda_{\parallel}$), and radial diffusivity ($\lambda_{\perp}$); 2. Kurtosis metrics: mean kurtosis (MK), axial ($K_{\parallel}$), and radial kurtosis ($K_{\perp}$)[11] (Figure 1), where MK is the average kurtosis over all diffusion directions, $K_{\parallel}$ is the kurtosis in the direction of the diffusion tensor eigenvector with the largest diffusion eigenvalue (typically along the direction of the axons), and $K_{\perp}$ is the average kurtosis over all directions perpendicular to the diffusion eigenvector with the largest eigenvalue (typically all directions perpendicular to the axons); 3. WMTI metrics: axonal water fraction (AWF), intra-axonal diffusivity (D_a), axial ($D_{e,\parallel}$), and radial

extra-axonal diffusivity ($D_{e,\perp}$). WMTI metrics were obtained from the DKI dataset in WM voxels consisting of aligned fiber bundles (defined here as FA ≥ 0.3)[14]. In the WMTI model, axonal fiber bundles are idealized as impermeable, cylindrical tubes, and the AWF represents the fraction of diffusion MRI-visible water contained within the tubes. Water within myelin is thus neglected, since it contributes little to the diffusion MRI signal due to its short T2 relaxation time. Qualitatively, the AWF can be regarded as an index of axonal fiber density. D_a is a measure of intrinsic diffusivity inside the axons. The remainder of the WM is modeled as the extra-axonal space, and $D_{e,\parallel}$ and $D_{e,\perp}$ are markers of changes in extra-axonal diffusivity.

Fiber tracking of the CST was performed using DSI Studio (http://dsi-studio.labsolver.org) using a generalized deterministic tracking algorithm that uses quantitative anisotropy as the termination index[18]. The CST was reconstructed as previously described[19] in accordance with the following steps. The tractography seed point was obtained by manually placing an ROI on each CST at the level of the rostral pons on the color-coded FA maps, and the tractography endpoint was obtained by manually placing a gray matter ROI on the ipsilateral precentral gyrus (anisotropy threshold = 0.2; angular threshold = 40°; step size = 1 mm; track length ≥ 50 mm; number of seeds = 10,000). The lesioned hemisphere CST could be reliably identified at the rostral pons in all subjects, even in patients with large infarctions. We added a logical “and” function so that only streamlines passing through both ROIs were included for further analysis. Fiber tracts were generated of the left and right CST. A neuroradiologist, blinded to demographic information and clinical data, visually inspected the CST tracts overlaid on the FA map for quality control purposes. Then, left and right CST tracks were converted to VOIs in native diffusion space. Average diffusion values of the CST VOIs were computed for all diffusion metrics and subjects using MATLAB. Lesioned hemisphere/contralateral hemisphere CST ratios were computed for all diffusion metrics.

Multi-slice VOIs of the infarct were identified by a neuroradiologist, blinded to demographic and clinical information, on the diffusion-weighted images with b-value of 2000 s/mm^2 by using the intensity filter module of MRICron (http://www.mccauslandcenter.sc.edu/crnl/mricron/). The volume of the infarct VOI, ipsilateral CST VOI, and the intersection between the CST and infarct VOIs were calculated using MRICron.

Statistical analyses were performed using Statistical Package for the Social Science (SPSS software version 22, Armonk, NY; IBM. Corp.). Comparisons of the ipsilateral and contralateral CST diffusion metrics were performed using the paired Wilcoxon Signed-Rank test. Associations between average CST diffusion metrics and 3-month FM-UE scale were evaluated using Spearman’s Rank Correlation tests. Results were considered significant when $p < 0.05$. Since this study was designed largely to be one of hypothesis generation, p-values were not corrected for multiple comparisons.

Results

Clinical Data

Twenty-one patients were recruited in this study. Subsequently, three patients were excluded because they were lost to follow-up and 3-month follow-up data were not available. One

patient was excluded because the DKI dataset was degraded by artifacts from bulk motion. Hence, seventeen patients were included in the analysis (Table 1). All patients received rehabilitation therapy (median number of days of therapy [SD] = 34 [18]). Overall, FM-UE score significantly improved between the baseline and the 3-month neurological examination ($p = 0.001$), with motor function improvement in 14 cases, no changes in 2 cases, and worsening function in 1 case. At 3 months, three patients had little if any UE motor function; five patients exhibited well-defined upper limb mass flexion and extension synergy-dependent movements; nine patients exhibited isolated upper limb movements. There was no significant correlation between the number of days of rehabilitation therapy and the baseline FM-UE score (r = − 0.340, $p = 0.181$) or the 3-month FM-UE score (r = − 0.373, $p = 0.140$).

Imaging Data

Please see Table 1 for details regarding infarct location and Table 2 for CST diffusion metrics. CST MD, FA, $\lambda_{||}$, $\lambda_{\perp}$, D_a, $D_{e,||}$, and $D_{e,\perp}$ were lower in the lesioned than contralateral hemisphere. MK and $K_{||}$ were greater in the lesioned than contralateral hemisphere CST. Table 3 demonstrates infarct volume, CST volume, their intersection, and diffusion metrics for the entire cohort, as well as for patients stratified based on the degree of recovery at 3 months. We found that there were significant correlations between the 3-month FM-UE scale, percent change of FM-UE between the baseline and 3-month visit, diffusion metrics of the lesioned hemisphere, and lesioned / contralateral hemisphere CST ratios (Table 4). The strongest associations were found between 3-month FM-UE and MK, and 3-month FM-UE and $K_{||}$, among kurtosis metrics, and between 3-month FM-UE and MD, among diffusivity metrics (Figure 2). We did not find any significant correlation between the number of days of rehabilitation therapy and kurtosis metrics. For example, there was no significant association between the number of days of rehabilitation therapy and lesional / contralateral MK (rho = 0.212, $p = 0.398$), $K_{||}$ (rho = 0.282, $p = 0.257$), MD (rho = − 0.318, $p = 0.198$), $\lambda_{||}$ (rho = − 0.330, $p = 0.181$), and FA (rho = − 0.78, $p = 0.759$).

Discussion

We conducted a prospective observational study designed to explore the hypothesis that DKI-derived metrics can be useful in assessing CST microstructural changes and predicting motor outcome after stroke. Due to the relatively small sample size, this proof-of-concept study is mainly for hypothesis generation, and our results will require validation in future studies with larger sample sizes. Both diffusivity and kurtosis diffusion metrics were able to detect early microstructural changes of the CST in the acute post-stroke phase, with larger differences between the ipsilateral and contralateral CST being observed for the kurtosis metrics. We also found moderately strong associations between motor outcome measured using the 3-month FM-UE scale and several of the diffusion metrics. The strongest motor outcome correlations were with MK (rho = −0.72) and $K_{||}$ (rho = −0.75) of the lesioned CST, and with lesioned / contralateral hemisphere CST MK (rho = −0.85) and $K_{||}$ (rho = − 0.78) ratios.

The observation of early CST diffusion changes is consistent with the known dynamics of acute neuronal damage after stroke, a phenomenon known as Wallerian degeneration[8]. In agreement with prior studies, we found that diffusivity metrics differed between the lesioned hemisphere CST and the contralateral CST[20], with greater acute – early subacute changes in $\lambda_{||}$ and MD compared to $\lambda_{\perp}$ 21. Kurtosis metrics, specifically MK, $K_{||}$, D_a, and $D_{e,||}$, were able to identify early microstructural changes of the CST. The kurtosis parameters provide microstructural information not available using conventional DTI [11], and it is important to assess whether the enhanced sensitivity to microstructural changes provided by DKI translates in improved motor outcome prediction. Larger absolute percent changes for kurtosis metrics than for diffusivity metrics have been consistently reported in ischemic stroke in the animal and human literature[13, 22, 23]. Here we find that kurtosis metrics also have greater sensitivity to the detection of CST microstructural alterations, as reflected by their larger absolute percent changes. For example, we found an average 12% increase in $K_{||}$ and an average 6.5% decrease in $\lambda_{||}$ of the ipsilateral compared to the contralateral CST. Absolute percent changes were larger along the axial direction than along the radial direction of the CST WM[24]. As expected, absolute percent changes of $\lambda_{||}$ and $K_{||}$ of the lesioned hemisphere CST were smaller than the absolute percent changes of $\lambda_{||}$ and $K_{||}$ of the core infarct, respectively 58% and −32% in a previous study[24]. The pathological correlates of increased MK in acute infarct and the downstream effect along the affected WM tracts are still incompletely understood. Acute infarct leading to early CST Wallerian degeneration may result in swelling or beading of downstream axons and dendrites[23–25]. Alternatively, ischemia could cause increased intra-axonal tortuosity, viscosity changes, microglia upregulation, mitochondrial or endoplasmatic reticulum changes, which may result in decreased D_a[22,23,26]. In agreement with Hui et al.[24], we found that the decrease in MD of the CST is mainly due to a drop in D_a, consistent with a proposed mechanism of axonal beading, although the CST $D_{e,||}$ was also decreased.

Previous studies have assessed the correlations between DTI-derived measures of CST integrity and functional motor impairment in acute stroke. Doughty et al. identified subtle changes in FA values of the CST in the vicinity of the lesion early after acute ischemic stroke; however, the degree of FA reduction did not significantly improve upon the predictive value of the baseline FM-UE scale for 3-month motor outcome[27]. Similarly, Puig et al. did not find significant correlations between 30-day motor outcome after stroke and CST FA measured in the pons in the acute phase, specifically less than 12 hours and 3 days post-stroke[10, 28]. Feng et al. developed the weighted CST lesion load, a novel imaging marker obtained by overlaying lesion maps obtained from DWI in the acute phase with a canonical CST[29]. The weighted CST lesion load was found to be a significant predictor of 3-month motor outcome. However, this metric is not a direct measure of CST injury and does not take into account CST pathophysiological changes after stroke. There is an unfulfilled clinical need for an early imaging marker of CST injury that would complement clinical assessment in the prediction of motor outcome and patient response to rehabilitation therapy. Our work demonstrates that DKI-derived diffusion metrics are able to detect early microstructural changes of the CST associated with acute stroke. Furthermore, DKI-derived metrics obtained in the acute phase show promising correlations with 3-month motor outcome. If these associations are validated in a future larger prospective study, then these

metrics may ultimately prove to be powerful adjuncts to clinical assessment in triaging patients who may benefit from neurorehabilitation treatment.

Stroke rehabilitative treatments are resource-intensive and patient selection is critical to identify individuals who are likely to benefit from the treatment[30]. Proposed motor outcome predictors, such as stroke location and volume[31], and degree of CST involvement[6, 29], may not provide adequate information to predict motor outcome and a significant amount of variance remains unexplained. Our results suggest that kurtosis metrics may prove valuable in determining motor pathway integrity. Specifically, we found that elevated MK / $K_{||}$ and decreased MD of the CST indicate a poor prognosis, and MK and $K_{||}$ had the strongest associations with the 3-month FM-UE scale. Patients with unfavorable diffusion markers may be less likely to benefit from motor rehabilitation programs. Although our preliminary observations will need confirmation in studies with larger cohorts, the use of imaging biomarkers of CST integrity could enable improved selection strategies in future stroke recovery trials.

This study has several limitations. We evaluated a small patient cohort, which limits our ability to evaluate the role of diffusion metrics in the context of other prognostic factors. On the other hand, it should be noted that all data were prospectively acquired, and imaging data were obtained using the same MR protocol and scanner. Future studies should include larger series of patients, which would allow one to determine whether the diffusion metrics are truly independent predictors of motor recovery, over and above the traditional clinical prognostic variables. We did not evaluate the subsequent temporal evolution of the observed CST diffusion measures. Furthermore, we included in the study patients with acute stroke and motor impairment regardless of the vascular territory involved. Our purpose was to evaluate the effects of acute ischemia on CST microstructure, regardless of where the core infarct was located along the motor pathways. This study design has been used in previous imaging-based studies on motor outcome after stroke[27,29].

In conclusion, our preliminary study reveals that early CST microstructural changes immediately following stroke can be detected using kurtosis metrics, specifically MK and $K_{||}$. We have preliminarily found strong associations between kurtosis metrics obtained at early time points after stroke and long-term motor outcome. A major limitation of this study is the small sample size; this study was designed largely to be one of hypothesis generation, and the usefulness of these imaging markers as independent predictors of disability in the context of other motor outcome predictors must be validated in future studies with larger sample sizes.

Acknowledgments

Grant Support

This project was supported, in part, by the South Carolina Clinical & Translational Research Institute (SCTR) at the Medical University of South Carolina, funded by the National Institutes of Health, National Center for Advancing Translational Science (Grant number UL1TR001450). Dr. Feng was supported by American Heart Association (14SDG1829003) and Drs. Feng, Bonilha and Kautz were supported by National Institute of Health (P20 GM109040).

We would like to acknowledge Rachael L. Deardorff for assisting with manuscript preparation.

Abbreviations

FM-UE	Upper Extremity Fugl-Meyer Motor Scale
CST	Corticospinal Tract
DKI	Diffusional Kurtosis Imaging
WMTI	White Matter Tract Integrity
FA	Fractional Anisotropy
MD	Mean Diffusivity
$\lambda_{\parallel}$	Axial Diffusivity
$\lambda_{\perp}$	Radial Diffusivity
MK	Mean Kurtosis
$K_{\parallel}$	Axial Kurtosis
$K_{\perp}$	Radial Kurtosis
AWF	Axonal Water Fraction
D_a	Intra-axonal Diffusivity
$D_{e,\parallel}$	Axial Extra-axonal Diffusivity
$D_{e,\perp}$	Radial Extra-axonal Diffusivity

References

1. Langhorne P, Coupar F, Pollock A. Motor recovery after stroke: a systematic review. The Lancet Neurology. 2009; 8:741–754. [PubMed: 19608100]
2. Hendricks HT, van Limbeek J, Geurts AC, et al. Motor recovery after stroke: a systematic review of the literature. Archives of physical medicine and rehabilitation. 2002; 83:1629–1637. [PubMed: 12422337]
3. Duncan PW, Goldstein LB, Matchar D, et al. Measurement of motor recovery after stroke. Outcome assessment and sample size requirements. Stroke; a journal of cerebral circulation. 1992; 23:1084–1089.
4. Prabhakaran S, Zarahn E, Riley C, et al. Inter-individual variability in the capacity for motor recovery after ischemic stroke. Neurorehabilitation and neural repair. 2008; 22:64–71. [PubMed: 17687024]
5. Ward NS, Newton JM, Swayne OB, et al. Motor system activation after subcortical stroke depends on corticospinal system integrity. Brain : a journal of neurology. 2006; 129:809–819. [PubMed: 16421171]
6. Puig J, Pedraza S, Blasco G, et al. Acute damage to the posterior limb of the internal capsule on diffusion tensor tractography as an early imaging predictor of motor outcome after stroke. AJNR American journal of neuroradiology. 2011; 32:857–863. [PubMed: 21474629]
7. Kumar P, Kathuria P, Nair P, et al. Prediction of Upper Limb Motor Recovery after Subacute Ischemic Stroke Using Diffusion Tensor Imaging: A Systematic Review and Meta-Analysis. Journal of stroke. 2016; 18:50–59. [PubMed: 26846758]

8. Yu C, Zhu C, Zhang Y, et al. A longitudinal diffusion tensor imaging study on Wallerian degeneration of corticospinal tract after motor pathway stroke. NeuroImage. 2009; 47:451–458. [PubMed: 19409500]
9. Groisser BN, Copen WA, Singhal AB, et al. Corticospinal tract diffusion abnormalities early after stroke predict motor outcome. Neurorehabilitation and neural repair. 2014; 28:751–760. [PubMed: 24519021]
10. Puig J, Pedraza S, Blasco G, et al. Wallerian degeneration in the corticospinal tract evaluated by diffusion tensor imaging correlates with motor deficit 30 days after middle cerebral artery ischemic stroke. AJNR American journal of neuroradiology. 2010; 31:1324–1330. [PubMed: 20299434]
11. Jensen JH, Helpern JA. MRI quantification of non-Gaussian water diffusion by kurtosis analysis. NMR in biomedicine. 2010; 23:698–710. [PubMed: 20632416]
12. Jensen JH, Helpern JA, Tabesh A. Leading non-Gaussian corrections for diffusion orientation distribution function. NMR in biomedicine. 2014; 27:202–211. [PubMed: 24738143]
13. Grinberg F, Ciobanu L, Farrher E, et al. Diffusion kurtosis imaging and log-normal distribution function imaging enhance the visualisation of lesions in animal stroke models. NMR in biomedicine. 2012; 25:1295–1304. [PubMed: 22461260]
14. Fieremans E, Jensen JH, Helpern JA. White matter characterization with diffusional kurtosis imaging. NeuroImage. 2011; 58:177–188. [PubMed: 21699989]
15. Fugl-Meyer AR, Jaasko L, Leyman I, et al. The post-stroke hemiplegic patient. 1. a method for evaluation of physical performance. Scandinavian journal of rehabilitation medicine. 1975; 7:13–31. [PubMed: 1135616]
16. Shelton FN, Reding MJ. Effect of lesion location on upper limb motor recovery after stroke. Stroke; a journal of cerebral circulation. 2001; 32:107–112.
17. Tabesh A, Jensen JH, Ardekani BA, et al. Estimation of tensors and tensor-derived measures in diffusional kurtosis imaging. Magnetic resonance in medicine : official journal of the Society of Magnetic Resonance in Medicine / Society of Magnetic Resonance in Medicine. 2011; 65:823–836.
18. Yeh FC, Verstynen TD, Wang Y, et al. Deterministic diffusion fiber tracking improved by quantitative anisotropy. PloS one. 2013; 8:e80713. [PubMed: 24348913]
19. Wakana S, Caprihan A, Panzenboeck MM, et al. Reproducibility of quantitative tractography methods applied to cerebral white matter. NeuroImage. 2007; 36:630–644. [PubMed: 17481925]
20. Moulton E, Amor-Sahli M, Perlbarg V, et al. Axial Diffusivity of the Corona Radiata at 24 Hours Post-Stroke: A New Biomarker for Motor and Global Outcome. PloS one. 2015; 10:e0142910. [PubMed: 26562509]
21. Bhagat YA, Hussain MS, Stobbe RW, et al. Elevations of diffusion anisotropy are associated with hyper-acute stroke: a serial imaging study. Magnetic resonance imaging. 2008; 26:683–693. [PubMed: 18440747]
22. Cheung JS, Wang E, Lo EH, et al. Stratification of heterogeneous diffusion MRI ischemic lesion with kurtosis imaging: evaluation of mean diffusion and kurtosis MRI mismatch in an animal model of transient focal ischemia. Stroke; a journal of cerebral circulation. 2012; 43:2252–2254.
23. Jensen JH, Falangola MF, Hu C, et al. Preliminary observations of increased diffusional kurtosis in human brain following recent cerebral infarction. NMR in biomedicine. 2011; 24:452–457. [PubMed: 20960579]
24. Hui ES, Fieremans E, Jensen JH, et al. Stroke assessment with diffusional kurtosis imaging. Stroke; a journal of cerebral circulation. 2012; 43:2968–2973.
25. Budde MD, Frank JA. Neurite beading is sufficient to decrease the apparent diffusion coefficient after ischemic stroke. Proceedings of the National Academy of Sciences of the United States of America. 2010; 107:14472–14477. [PubMed: 20660718]
26. Weber RA, Hui ES, Jensen JH, et al. Diffusional kurtosis and diffusion tensor imaging reveal different time-sensitive stroke-induced microstructural changes. Stroke; a journal of cerebral circulation. 2015; 46:545–550.

27. Doughty C, Wang J, Feng W, et al. Detection and Predictive Value of Fractional Anisotropy Changes of the Corticospinal Tract in the Acute Phase of a Stroke. Stroke; a journal of cerebral circulation. 2016; 47:1520–1526.

28. Puig J, Blasco G, Daunis IEJ, et al. Decreased corticospinal tract fractional anisotropy predicts long-term motor outcome after stroke. Stroke; a journal of cerebral circulation. 2013; 44:2016–2018.

29. Feng W, Wang J, Chhatbar PY, et al. Corticospinal tract lesion load: An imaging biomarker for stroke motor outcomes. Annals of neurology. 2015; 78:860–870. [PubMed: 26289123]

30. Stinear C. Prediction of recovery of motor function after stroke. The Lancet Neurology. 2010; 9:1228–1232. [PubMed: 21035399]

31. Chen CL, Tang FT, Chen HC, et al. Brain lesion size and location: effects on motor recovery and functional outcome in stroke patients. Archives of physical medicine and rehabilitation. 2000; 81:447–452. [PubMed: 10768534]

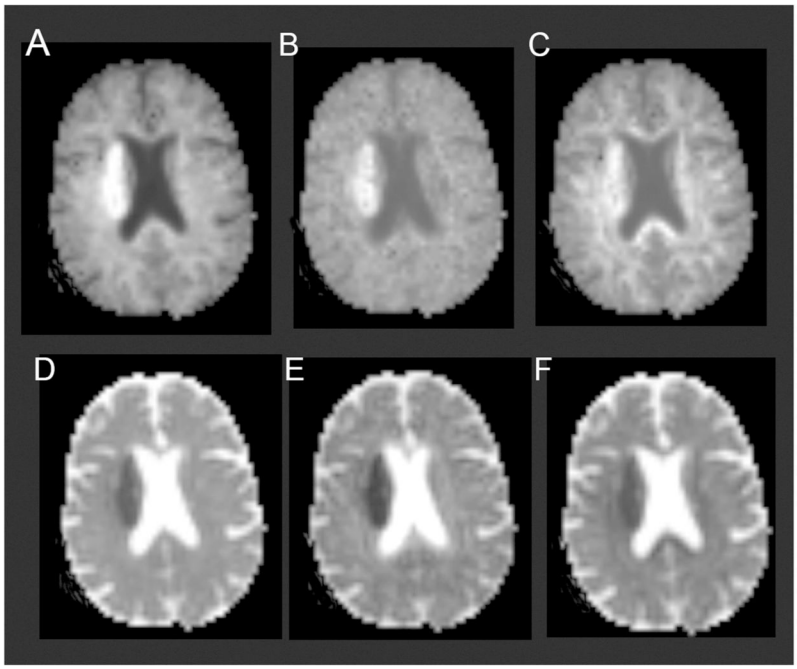

Figure 1.

(A) Mean kurtosis, (B) axial kurtosis, (C) radial kurtosis, (D) mean diffusivity, (E) axial diffusivity, (F) radial diffusivity maps obtained from the DKI dataset in a representative patient with acute ischemic infarct of the right corona radiata.

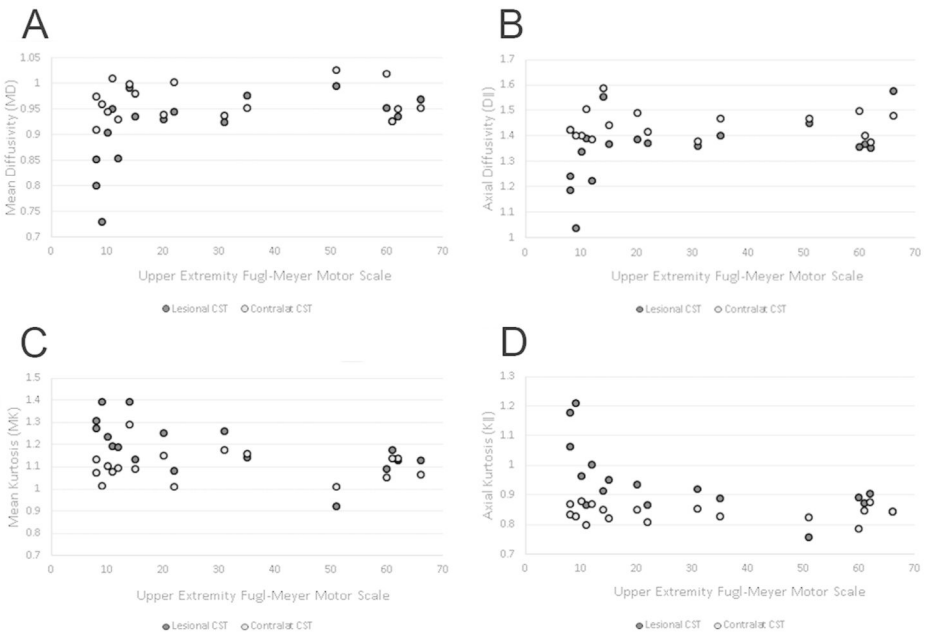

Figure 2.

Scatter plots for Upper Extremity Fugl-Meyer Motor Scale versus (A) mean diffusivity, (B) axial diffusivity, (C) mean kurtosis, and (D) axial kurtosis of the corticospinal tracts.

Table 1

Patient Clinical Characteristics

Demographics (N =17)	
Age (yrs) *	55.7 (12.3)
Males	64.7%
Race (Caucasian / African American)	12 / 5
Lesion side (Right)	70.6%
Stroke Etiology	
Small Vessel Disease	35.3%
Cardioembolism	17.6%
Large Vessel Atherosclerosis	29.4%
Unknown	17.6%
r-tPA or Reperfusion Therapy	41.2%
Hypertension	82.4%
Diabetes Mellitus	35.3%
Dyslipidemia	70.6%
Atrial Fibrillation	23.5%
Coronary artery disease	11.8%
Antiplatelet use	88.2%
Anticoagulation use	17.6%
Statin on Discharge	82.3%
Smoking on admission	47.1%
Length of hospital stay (days) *	5.8 (3.8)
Clinical Assessment	
Days between stroke onset and MRI *	2.0 (1.0)
Days from stroke onset to baseline assessment *	2.6 (1.5)
Days from admission to follow up visit *	94.1 (9.6)
Median number of days of rehabilitation therapy	34 (18.1)
Baseline NIHSS	11.2 (6.5)
3-month NIHSS	4.9 (3.9)
Baseline FM-UE *	19.1 (16.9)
3-month FM-UE *	29.1 (22.0)
Median 3-month mRS (Range)	3 (1–4)
Location of Infarction	**N (%)**
Right Hemisphere	12 (70.5)
Left Hemisphere	5 (29.5)
Motor Cortex	6 (35.3)
Premotor Cortex	5 (29.5)
Centrum Semiovale	4 (23.5)
Corona Radiata	9 (52.9)
Posterior Limb Internal Capsule	9 (52.9)

Brain Stem	4 (23.5)

*Mean (SD)

FM = Fugl-Meyer Motor Scale; UE = Upper extremity.

Table 2

Diffusion Metrics of Lesioned and Contralateral Corticospinal Tract in Stroke with Motor Impairment

Diffusion Metric	**Lesioned CST***	**Contralat CST***	***p - value***
Mean Diffusivity	0.91 (0.07)	0.96 (0.03)	0.003
Axial Diffusivity	1.35 (0.12)	1.44 (0.06)	0.002
Radial Diffusivity	0.70 (0.05)	0.72 (0.04)	0.031
Fractional Anisotropy	0.41 (0.03)	0.43 (0.03)	0.025
Mean Kurtosis	1.19 (0.12)	1.10 (0.07)	0.002
Axial Kurtosis	0.94 (0.11)	0.84 (0.03)	0.001
Radial Kurtosis	1.48 (0.18)	1.43 (1.13)	0.193
Axonal Water Fraction	0.41 (0.02)	0.40 (0.02)	0.246
Intra-axonal Diffusivity	0.71 (0.09)	0.78 (0.06)	0.001
Extra-axonal Axial Diffusivity	1.95 (0.17)	2.05 (0.10)	0.002
Extra-axonal Radial Diffusivity	1.07 (0.07)	1.10 (0.05)	0.049

*Mean (SD)

Table 3

Volumetric and Corticospinal Tract Diffusion Metrics in the Entire Cohort and in Subgroups of Patients Stratified Based on the 3-Month Motor Outcome

		Entire Cohort (N = 17)	FM-UE ≤ 9 (N= 3)	FM-UE 10–18 (N = 5)	FM-UE > 18 (N = 9)
Infarct Volume *		43.7 (62.5)	139.1 (86.9)	34.8 (43.6)	16.9 (26.7)
CST Volume *		4.1 (3.0)	6.3 (4.4)	3.0 (2.2)	3.4 (2.9)
Intersection infarct-CST *		1.1 (1.5)	3.4 (2.5)	0.9 (1)	0.4 (0.2)
Mean Diffusivity	Lesioned CST	0.91 (0.07)	0.79 (0.06)	0.92 (0.05)	0.94 (0.02)
	Ratio **	0.95 (0.06)	0.84 (0.07)	0.95 (0.03)	0.98 (0.03)
Axial Diffusivity	Lesioned CST	1.35 (0.12)	1.15 (0.11)	1.37 (0.11)	1.40 (0.07)
	Ratio	0.93 (0.07)	0.81 (0.07)	0.94 (0.04)	0.97 (0.04)
Radial Diffusivity	Lesioned CST	0.70 (0.05)	0.61 (0.04)	0.70 (0.02)	0.72 (0.03)
	Ratio	0.96 (0.07)	0.87 (0.08)	0.97 (0.02)	0.99 (0.06)
Fractional Anisotropy	Lesioned CST	0.41 (0.03)	0.39 (0.03)	0.42 (0.03)	0.41 (0.04)
	Ratio	0.96 (0.07)	0.90 (0.05)	0.96 (0.04)	0.98 (0.08)
Mean Kurtosis	Lesioned CST	1.19 (0.12)	1.32 (0.06)	1.22 (0.10)	1.13 (0.10)
	Ratio	1.08 (0.10)	1.24 (0.12)	1.09 (0.03)	1.03 (0.06)
Axial Kurtosis	Lesioned CST	0.94 (0.11)	1.15 (0.08)	0.94 (0.05)	0.88 (0.05)
	Ratio	1.12 (0.13)	1.36 (0.09)	1.11 (0.04)	1.05 (0.06)
Radial Kurtosis	Lesioned CST	1.48 (0.18)	1.53 (0.15)	1.57 (0.21)	1.42 (0.18)
	Ratio	1.04 (0.10)	1.13 (0.16)	1.07 (0.06)	0.99 (0.08)
Axonal Water Fraction	Lesioned CST	0.41 (0.02)	0.42 (0.01)	0.42 (0.02)	0.39 (0.02)
	Ratio	1.02 (0.05)	1.06 (0.06)	1.04 (0.02)	0.99 (0.03)
Intra-axonal Diffusivity	Lesioned CST	0.71 (0.09)	0.59 (0.08)	0.73 (0.07)	0.73 (0.07)
	Ratio	0.91 (0.09)	0.77 (0.07)	0.95 (0.05)	0.93 (0.06)
Axial Extra-axonal Diffusivity	Lesioned CST	1.95 (0.17)	1.71 (0.14)	2.00 (0.20)	2.00 (0.11)
	Ratio	0.95 (0.06)	0.86 (0.05)	0.95 (0.04)	0.97 (0.04)
Radial Extra-axonal Diffusivity	Lesioned CST	1.07 (0.07)	0.95 (0.06)	1.10 (0.66)	1.09 (0.03)
	Ratio	0.97 (0.05)	0.89 (0.04)	0.98 (0.03)	0.99 (0.05)

* In ml.

** Lesioned hemisphere / contralateral hemisphere CST

Table 4

Correlations between Baseline Fugl-Meyer Upper-Extremity Scale, Corticospinal Tract Diffusion Metrics, and 3-month Fugl-Meyer Upper-Extremity Scale

	Rho	***p*-value**		
Baseline vs. 3-mo FM-UE	**0.80**	**<0.001**	**0.80**	
	Lesioned Hemisphere CST		**Lesioned/Contralateral CST Ratio**	
	Rho	***p*-value**	**Rho**	***p*-value**
3-month FM-UE				
Mean Diffusivity	0.65	0.007	0.69	0.002
Axial Diffusivity	0.55	0.022	0.73	0.001
Radial Diffusivity	0.53	0.030	0.60	0.011
Fractional Anisotropy	0.08	0.761	0.40	0.111
Mean Kurtosis	−0.72	0.001	−0.85	<0.001
Axial Kurtosis	−0.75	0.001	−0.78	<0.001
Radial Kurtosis	−0.33	0.196	−0.47	0.056
Axonal Water Fraction	−0.45	0.072	−0.63	0.007
Intra-axonal Diffusivity	0.51	0.035	0.48	0.054
Axial Extra-axonal Diffusivity	0.45	0.070	0.61	0.009
Radial Extra-axonal Diffusivity	0.37	0.142	0.45	0.072
% change of FM-UE				
Mean Diffusivity	0.64	0.006	0.47	0.055
Axial Diffusivity	0.49	0.046	0.66	0.004
Radial Diffusivity	0.69	0.002	0.42	0.098
Fractional Anisotropy	−0.01	0.974	0.47	0.060
Mean Kurtosis	−0.61	0.010	−0.72	0.001
Axial Kurtosis	−0.65	0.005	−0.65	0.004
Radial Kurtosis	−0.28	0.269	−0.48	0.049
Axonal Water Fraction	−0.54	0.026	−0.59	0.013
Intra-axonal Diffusivity	0.42	0.095	0.43	0.083
Axial Extra-axonal Diffusivity	0.42	0.090	0.56	0.019
Radial Extra-axonal Diffusivity	0.53	0.028	0.24	0.349